IVYSPRING INTERNATIONAL PUBLISHER

Nanotheranostics

2017; 1(4): 440-449. doi: 10.7150/ntno.21905

Research Paper

Ultrasound-Stimulated Drug Delivery Using Therapeutic Reconstituted High-Density Lipoprotein Nanoparticles

Fangyuan Xiong[1, 2], Sabnis Nirupama[3], Shashank R Sirsi[1, 4], Andras Lacko[3], Kenneth Hoyt[1, 4]✉

1. Department of Bioengineering, University of Texas at Dallas, Richardson, TX 75080 USA.
2. Department of Medical Ultrasound, Tongji Hospital of Tongji Medical College, Huazhong University of Science and Technology, Wuhan, China.
3. Department of Pediatrics, University of North Texas Health Sciences Center, Fort Worth TX 76107 USA;
4. Department of Radiology, University of Texas Southwestern Medical Center, Dallas, TX 75390 USA.

✉ Corresponding author: Kenneth Hoyt, PhD. MBA. FAIUM. University of Texas at Dallas, BSB 13.929, 800 W Campbell Rd, Richardson, TX 75080 USA. Ph: (972) 883-4958 Fax: (972) 883-2088 Email: kenneth.hoyt@utdallas.edu

Received: 2017.07.16; Accepted: 2017.10.09; Published: 2017.11.01

Abstract

The abnormal tumor vasculature and the resulting abnormal microenvironment are major barriers to optimal chemotherapeutic drug delivery. It is well known that ultrasound (US) can increase the permeability of the tumor vessel walls and enhance the accumulation of anticancer agents. Reconstituted high-density lipoproteins (rHDL) nanoparticles (NPs) allow selective delivery of anticancer agents to tumor cells via their overexpressed scavenger receptor type B1 (SR-B1) receptor. The goal of this study is to investigate the potential of noninvasive US therapy to further improve delivery and tumor uptake of the payload from rHDL NPs, preloaded with an infrared dye (IR-780), aimed to establish a surrogate chemotherapeutic model with optical localization. Athymic nude mice were implanted orthotopically with one million breast cancer cells (MDA-MB-231/Luc). Three weeks later, animals were divided into seven groups with comparable mean tumor size: control, low, moderate, and high concentration of rHDL NPs alone groups, as well as these three levels of rHDL NPs plus US therapy groups (N = 7 to 12 animals per group), where low, moderate and high denote 5, 10, and 50 μg of the IR-780 dye payload per rHDL NP injection, respectively. The US therapy system included a single element focused transducer connected in series with a function generator and power amplifier. A custom 3D printed cone with an acoustically transparent aperture and filled with degassed water allowed delivery of focused US energy to the tumor tissue. US exposure involved a pulsed sequence applied for a duration of 5 min. Each animal in the US therapy groups received a slow bolus co-injection of MB contrast agent and rHDL NPs. Animals were imaged using a whole-body optical system to quantify intratumoral rHDL NP accumulation at baseline and again at 1 min, 30 min, 24 h, and 48 h. At 48 h, all animals were euthanized and tumors were excised for *ex vivo* analysis. We investigated a noninvasive optical imaging method for monitoring the effects of US-stimulated drug delivery of IR-780 dye-loaded rHDL NPs in living animals. No change in optical imaging data was found in the control animals. However, there was considerable dye accumulation (surrogate drug) within 48 h in the low (5 μg), moderate (10 μg), and high (50 μg) rHDL NP concentration-dosed group animals ($p < 0.09$). With US therapy added to the experimental protocol, there was an additional and significant increase in local tumor drug uptake at 48 h ($p < 0.02$). Optical image data collected from *ex vivo* tumor samples confirmed tumor retention of the IR-780 dye-loaded rHDL NPs and correlated positively with *in vivo* optical imaging results ($R^2 > 0.69$, $p < 0.003$). IR-780 dye extraction from the tumor tissue samples confirmed the *in vivo* and *ex vivo* US therapy findings. Overall, the addition of US therapy considerably improved local rHDL NP accumulation in tumor tissue. This study concludes that US-mediated drug delivery can facilitate tumor uptake of rHDL NPs and more research is warranted to optimize the drug dosing schedule and the respective therapeutic protocols.

Key words: cancer, drug delivery, microbubble contrast agents, nanoparticles, ultrasound.

Introduction

Physiological barriers in cancerous tissue can limit the effective systemic delivery of chemotherapeutic drugs. While the tumor vasculature is known to be leaky, vascular permeability of these tumors exhibit spatial and temporal heterogeneity (1) thus, limiting the therapeutic response via the extravasation of drugs from hypopermeable tumor vessels and those with compromised blood flow. Accordingly, the tumor vasculature serves as a major barrier to optimal drug delivery (2).

It has been well established that noninvasive ultrasound (US) can safely and reversibly increase the permeability of the tumor vessel walls and to temporarily enhance the accumulation of anticancer drugs (3-6) and gene therapy vectors (7-9) in the surrounding diseased tissues. These US-based approaches are facilitated using microbubble (MB) contrast agents, (mean diameter < 5 μm). Using acoustic pressures as low as a few hundred kilopascals (kPa), once the US waves encounter circulating MBs they induce a large proportion of the MB population to resonate (termed stable cavitation) resulting in the mechanical separation of endothelial cells and the desired enhanced microvascular permeabilization (10). While MB exposure to higher acoustic pressures may also enhanced microvascular permeability via the effects of inertial cavitation, the likelihood of compromised blood flow in the tumor due to microvascular damage is also more likely. Obviously, this latter situation would impede delivery of any circulating anticancer drug and as such should be avoided.

From use of several different xenograft tumor models, it has been shown that low pressure US-stimulated drug delivery (also termed US therapy), enhances the efficacy of drug treatment of tumors, compared to systemic injection of the drugs alone (4, 5, 11). Specifically, use of US-stimulated drug delivery significantly enhanced the anticancer response in tumor-bearing animals, dosed with either low molecular weight (cisplatin) or high molecular weight (cetuximab) drugs (neoadjuvant therapy) (5). It has also been demonstrated that US-stimulated drug delivery is a promising tool for improved treatment of residual cancer cells that remain after surgical resection of the primary tumor (adjuvant therapy) (11). In a recent pilot study, involving 10 patients with inoperable pancreatic cancer, Kotopoulis et al. (12, 13), showed that continuous US exposure of FDA-approved MBs and a standard chemotherapeutic drug (gemcitabine) at the tumor site can prolong patient survival. This, pioneering study employed US-stimulated drug delivery, for the first time, for the treatment of cancer patients.

High-density lipoproteins (HDL) are a class of nanoparticles (NPs) that help transport cholesterol from peripheral tissues to the liver. The unique structure of HDL makes it ideally suited for the transport of lipophilic compounds in its core compartment so that the payload can safely reach its destination (14). The same advantages apply to the transport of other lipophilic payloads, such as anticancer drugs (15, 16). Despite promising findings, the use of native plasma lipoproteins as drug carriers has been limited by the lack of a consistent composition so significant research activity has been committed to developing synthetic, or reconstituted HDL (rHDL), NPs as drug delivery vehicles (17-19). Of importance, the payload of both native and synthetic HDL NPs is known to be primarily delivered by scavenger receptor type B1 (SR-B1)-mediated endocytosis (20, 21). Note that SR-B1 is overexpressed in cancer cells compared to normal cell types (19). It has been hypothesized that SR-B1 overexpression is linked to a cancer cells need for cholesterol as demanded by their high rate of proliferation (22). Therefore, rHDL NPs allow selective delivery of anticancer agents to cancer cells via the SR-B1 receptor when injected systemically, thus locally unloading the drug payload from NPs selectively to tumor tissue. Notwithstanding, any adjunct targeting strategy that could noninvasively enhance rHDL NP extravasation at the tumor site would improve drug delivery and potentially help maximize any therapeutic response. IR-780 iodide is a lipophilic, near-IR NIR) fluorescence imaging heptamethine cyanine dye, with a peak emission at 780 nm, which has gained interest in recent years due to its superior tumor targeting and imaging potential (23, 24). Although its hydrophobic property limits its clinical use, it is a useful candidate for mimicking lipophilic drug delivery mediation via the rHDL modality. Additionally, IR-780 dye is associated with preferential accumulation and longer retention in certain cancer cells, including breast cancer and lung cancer, compared to other NIR dyes (25). In this paper, we detail the use of US-stimulated drug delivery to locally enhance the payload of NIR dye uptake from rHDL NPs by tumor tissue, using an orthotopic breast cancer murine model.

Materials and Methods

Cell lines and culture methods

Luciferase-positive human breast cancers cells (MDA-MB-231/Luc, Cell Biolabs, San Diego, CA, USA) were maintained in L-15 Leibovitz medium (Hyclone, Logan, UT, USA) supplemented with 10%

fetal bovine serum. All cells were cultured to approximately 70 to 90% confluency before passaging and grown at 37°C without CO_2 (Heracell 150i, Thermo Fisher Scientific, Waltham, MA, USA). Appropriate cell numbers were determined using a digital cell counting instrument (Countess II Automated Cell Counter, Thermo Fisher Scientific).

rHDL NP assembly

The rHDL NPs containing an imaging dye IR-780 (Sigma Aldrich, St. Louis, MO, USA) were prepared via the cholate dialysis procedure (26, 27). To a glass vial, 7.5 mg/mL of phosphatidylcholine, 0.175 mg/mL of free cholesterol, and 0.075 mg/mL of cholesterol oleate, (all from Sigma Aldrich) were added from stock solutions in chloroform and mixed thoroughly. This mixture was then dried under nitrogen. To this mixture, 0.75 mg/mL IR-780 from a stock prepared in dimethyl sulfoxide (DMSO) (Sigma Aldrich) and 30 µL/mL DMSO were added, followed by 2.5 mg/mL Apolipoprotein A-I (MC Lab, San Francisco, CA, USA). The mixture was then vortexed before adding 7.5 mg/mL of sodium cholate. A buffer solution (10 mM Tris, 0.1 M potassium chloride, 1 mM EDTA pH 8.0) was used to make up the desired volume. The solution was mixed thoroughly and incubated on a rotary shaker at 4 °C for 12 hours. The formulation was then dialyzed against 2 L of 1x phosphate buffered saline for 48 h at 4 °C, with a change of buffer 3 times every 2 h on the first day, and later change of buffer after every 12 h. The mixture was centrifuged at 239.4 g for 1 min and the supernatant was filtered through a 0.45 µM filter (EMD Millipore, Billerica, MA, USA), aliquoted and stored at -20 °C until used. Dye incorporation into the rHDL NPs was quantified by absorbance measurements at 780 nm (Synergy HT, BioTek, Winooski, VT, USA). The hydrodynamic diameter of the rHDL NPs was estimated using a submicron particle size analyzer (Delsa Nano, Beckman Coulter, Brea, CA). An average of 70 runs was captured by the machine and the number distribution of average particle size was reported. The final size of the rHDL NPs was found to 44.8 ± 24 nm.

Animal studies

All animal experiments were reviewed and approved by the Institutional Animal Care and Use Committee at the University of Texas at Dallas. Four-week-old female athymic mice (Charles River Laboratories, Wilmington, MA, USA) were implanted orthotopically in the right inguinal mammary fat pad area with 1 million breast cancer cells. Implanted tumors grew for three to four wk and were physically measured biweekly throughout using digital calipers. Thereafter, animals were divided in experimental groups so that mean group tumor size was comparable. These group assignments were: randomly assigned to one of seven groups: control, low concentration of rHDL NPs ± US therapy, moderate concentration of rHDL NPs ± US therapy, high concentration of rHDL NPs ± US therapy (N = 7 to 12 animals per group) where low, moderate and high signifies 5, 10, and 50 µg of IR-780 dye-loaded rHDL NPs per injection, respectively. During all procedures, animals were placed on a heating pad to maintain core temperature and controlled with 2 to 3% isoflurane anesthesia (V3000PK, Parkland Scientific, Coral Springs, FL, USA).

US-stimulated drug delivery

Our US therapy system and setup comprised of a single element focused immersion transducer (V392-SU-F, Olympus, Waltham, MA, USA) electronically placed in series with a digital signal generator (AFG3002B, Tektronix, Beaverton, OR, USA) and power amplifier (A075, Electronics & Innovation, Rochester, NY, USA), Figure 1. The US transducer had the following characteristics: 1.0 MHz center frequency, 1.5" diameter and © US exposure involved a 100-cycle pulse sequence transmitted with a peak negative pressure of 0.45 MPa that was repeated every 10 ms for a duration of 5 min. A custom transducer cone was created using 3-dimensional (3D) printing of a rigid polymer material. This cone allowed secure insertion of the transducer face whereas the narrowed distal end comprised of an open acoustic aperture just proximal to the transducer focal position that was covered with acoustically transparent polystyrene film (McMaster-Carr, Douglasville, GA, USA). Once assembled, this transducer cone was filled with degassed water to allow coupling of US energy to tissue placed beyond the aperture, Figure 2. The acoustic output in the transducer focus was sensitively measured or confirmed using a hydrophone scanning system (AIMS III, Onda Corp, Sunnyvale, CA, USA). The US focus extended approximately 1 cm beyond the aperture face allowing delivery (penetration) of US energy in the target tissue at depth.

After placement of a 27G x ½" winged infusion catheter (Terumo Corp, Hatagaya, Tokyo, Japan) in the tail vein, each animal received a slow bolus co-injection of MB contrast agent (100 µL, Definity, Lantheus Medical Imaging, North Billerica, MA, USA) and concentrated rHDL NPs diluted to 150 µL with 0.9% sodium chloride diluent (Hospira, Lake Forest, IL, USA). Immediately thereafter, a single session of US or sham therapy was applied to the tumor tissue

after coupling the water-backed polystyrene-coated acoustic aperture with US transmission gel (Aquasonic 100, Parker Laboratories, Fairfield, NJ, USA). Throughout each US-stimulated drug delivery session, the US transducer was positioned and slowly moved about the tumor by hand. By employing a continuous raster scan approach throughout the entire US exposure period, the likelihood of complete (spatial) tumor treatment was maximized. Note that the MB concentration used for US therapy was 300-fold larger than that used for a typical diagnostic contrast-enhanced US examination in human (28).

In vivo and *ex vivo* optical imaging

Since the rHDL NPs were preloaded with IR-780 dye, optical imaging of live animals was employed to quantify rHDL tumor update and retention at baseline and again at 1 min, 30 min, 24 h, and 48 h after receiving rHDL NPs ± US therapy exposure. Thereafter, all animals were humanely euthanized via isoflurane overdose and cervical dislocation. Tumors were resected, rinsed with saline, weighed, and then placed in translucent 6-well plates (Thermo Fisher Scientific). Optical imaging was performed using a dedicated small animal optical imaging system (Pearl Trilogy, LI-COR Biotechnology, Lincoln, NE, USA). In addition to white light imaging for animal visualization, co-registered fluorescence imaging was performed using the 800-nm channel excited at a wavelength of 785 nm and emitting at 820 nm. The ability to image tumors over time allows *in vivo* optical measurement of local fluorescence tracer uptake and any US therapy-induced bioeffects (3). Fluorescent signal intensity from a user-defined region-of-interest (ROI) encompassing the *in vivo* or *ex vivo* tumor mass was quantitatively measured using software provided by the vendor (Image Studio Software, LI-COR Biotechnology) and normalized by background region. All ROIs were manually placed around each tumor using the white light image for guidance. The same ROI was then used to quantify tumor fluorescence as a mean signal intensity measurement.

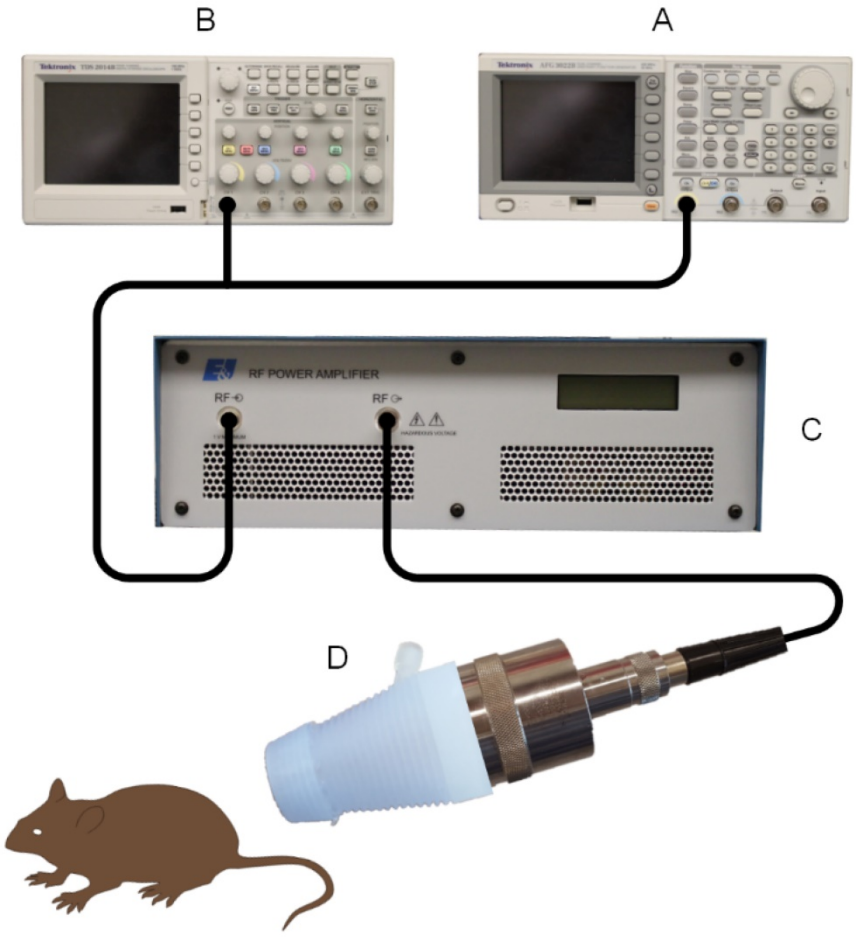

Figure 1. Custom ultrasound (US)-stimulated drug delivery system comprised of an (A) arbitrary function generator and (B) digital oscilloscope in series with a (C) power amplifier and (D) focused single element transducer. A water-filled 3-dimensional (3D) printed polymer cone with an acoustically transparent aperture is placed on the transducer face for coupling US energy in the focus with the target tissue of interest.

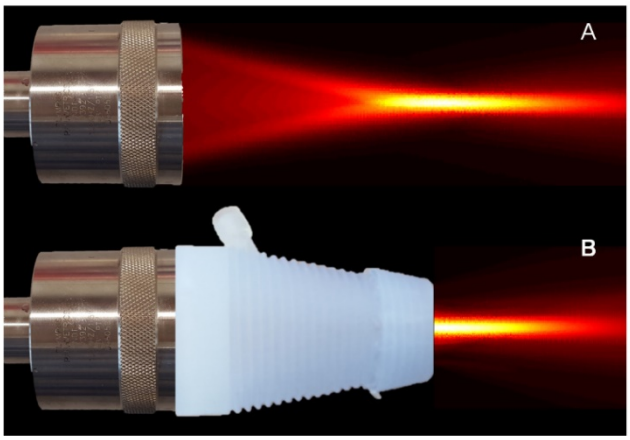

Figure 2. US therapy transducer (A) before and (B) after being placed with a 3D printed cone with an acoustically transparent aperture is placed on the transducer face for coupling US energy in the focus with the target tissue of interest. High-resolution spatial maps of US pressure (transducer output) confirms acoustic coupling and no field aberration.

Tumor tissue dye extraction

Excised tumors were cut into small pieces, rinsed with saline, and then weighed. These pieces were transferred to 1.5 mL microcentrifuge tubes supplemented with a 1.0 mL radioimmunoprecipitation assay buffer comprised of 50 mM Tris-base (pH 7.4), 150 mM sodium chloride (NaCl), 1% Triton X-100, 0.5% sodium deoxycholate, and 0.1% sodium dodecyl sulfate (SDS). Tissue samples were homogenized by ceramic beads (Mo Bio, Carlsbad, CA, USA) using mechanical agitation (Vialmix, Lantheus Medical Imaging). After centrifugation at 2000 g for 10 min (repeated twice), the supernatants were transferred to a 96-well black plate (200 µL per well). Each tissue sample was measured in triplicate. A standard curve was produced by allocating the rHDL NPs and control tumor lysate at different doses. The fluorescence signal from each well was quantified by a microplate reader (Synergy H4, BioTek) with optical excitation and emission set at 780 nm and 820 nm, respectively. Tumor uptake of the IR-780 dye was calculated as the amount of dye material in each tumor normalized by the injected dose and reported as a percentage.

Statistical analysis

All experimental data was summarized as the mean ± standard error. A repeated-measures analysis of variance (ANOVA) test was used to assess longitudinal trends in the *in vivo* optical imaging group data. Differences in rHDL NP delivery with and without the use of US therapy were evaluated using a Mann-Whitney test. Relationships between *in vivo* and *ex vivo* optical imaging data were analyzed using a Pearson correlation test. A two-sample *t*-test was utilized to evaluate differences in initial tumor size (baseline) and excised tumor mass weight. A *p*-value of less than 0.05 was considered statistically significant. A Bonferroni correction was used to counteract multiple comparisons. All analyses were completed using statistical software (JMP 12, SAS Institute Inc, Cary, NC, USA).

Results

At baseline and immediately preceding initiation of the US-stimulated drug delivery study, animals in all groups developed comparably sized tumors ranging from 680.4 ± 111.5 to 760.6 ± 62.1 ($p > 0.10$), Figure 3. Following baseline optical imaging to detect presence of any background fluorescence signal from the tumor tissue, animals received: sham treatment (control), low concentration of rHDL NPs ± US therapy, moderate concentration of rHDL NPs ± US therapy, or high concentration of rHDL NPs ± US therapy where low, moderate and high signifies a single injection of either 5, 10, or 50 µg of IR-780 dye-loaded rHDL NPs. Thereafter, whole body optical imaging was repeated at 1, 30, and 60 min, and again at 24 and 48 h. A representative sequence of optical images is presented in Figure 4. Note the progressive accumulation of the rHDL NPs in tumor tissue as a function of both time and injected concentration. One can also appreciate how the incorporation of US therapy improves delivery of the rHDL NPs. For the moderate and high rHDL NP concentrations, these phenomena are captured in the *in vivo* optical images as early as 30 min after administration. Note the perceived reduction in the optical signal from the liver in the high concentration rHDL NP group animals. This observation was simply due to the increased image scale necessary to show actual variations in the tumor tissue and does not represent a real biological phenomenon.

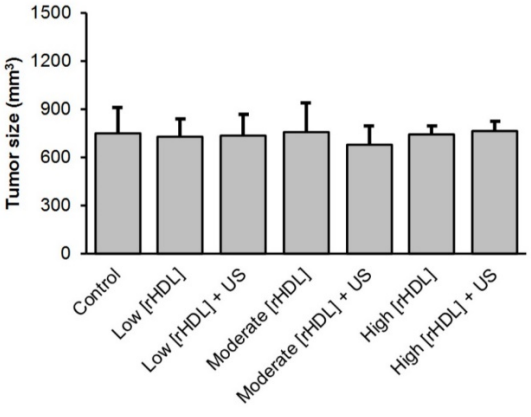

Figure 3. Summary of tumor sizes at baseline for the control, low concentration reconstituted high-density lipoprotein (rHDL, low [rHDL]) ± US therapy, moderate [rHDL] ± US therapy, or high [rHDL] ± US therapy group animals.

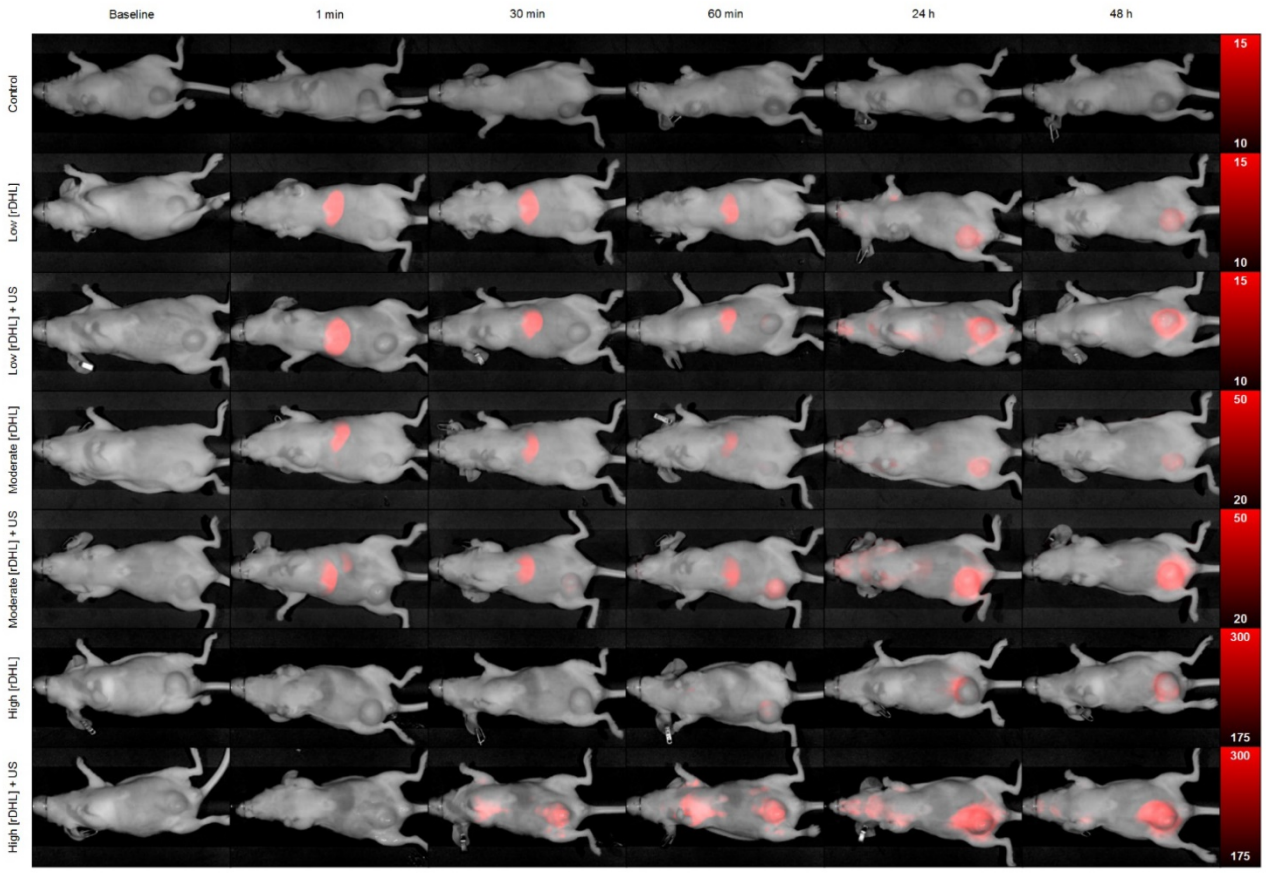

Figure 4. Representative *in vivo* optical images of breast tumor-bearing animals administered a single dose of either control (sham), low [rHDL] ± US therapy, moderate [rHDL] ± US therapy, or high [rHDL] ± US therapy at baseline, 1 min, 30 min, 60 min, 24 h and 48 h. Note the different optical image intensity (colorbar) ranges for each animal group.

Longitudinal *in vivo* optical imaging data from the US-stimulated drug delivery study is summarized in Figure 5. A repeated measures ANOVA revealed that no changes in the *in vivo* optical signal was found in the control animals ($p = 0.32$), however, there was a significant change during the same observation time in the low and moderate rHDL NP concentration-dosed animals ($p < 0.002$) and a trend towards significance in animals administered a high concentration of rHDL NPs ($p = 0.09$). With US therapy added to the experimental protocol, a significance change over time and within 48 h was also noted in the low and moderate concentration rHDL NP-dosed animals ($p < 0.001$) in addition to the high concentration rHDL NP-dosed animals ($p = 0.02$). When comparing same day *in vivo* optical imaging data from animals administered rHDL NPs ± US therapy revealed no significant differences for those receiving the low concentration injections and only at 24 and 48 h for the high concentration-dosed animals ($p < 0.04$). Noteworthy, animals administered the moderate rHDL NPs ± US therapy exhibited significant differences in tumor uptake (dye accumulation) as early as 30 min after treatment ($p < 0.01$). These same day tumor measurements further confirm that US therapy can significantly improve delivery of systemically injected rHDL NPs.

After *in vivo* optical imaging at the 48-h time point, animals were humanely euthanized. Regardless of experimental group, no differences were found between any of the excised tumor weights ($p > 0.08$). A comparison of *ex vivo* optical image data of excised tumor samples to *in vivo* optical measurements obtained immediately prior to euthanasia reveals a strong positive correlation for all animals receiving rHDL NPs ± US therapy ($R^2 > 0.69$, $p < 0.003$) but not those in the control group ($R^2 = 0.09$, $p = 0.52$). Evident from the data plotted in Figure 6, US-stimulated drug delivery enhances rHDL NP accumulation in the target tumor tissue compared to rHDL NP injection alone and trends observed appear independent of dose concentration.

Tumor samples were further processed to extract the IR-780 dye that was preloaded into the rHDL NPs and to provide an additional measure of target tissue drug accumulation. A comparison of group data from animals administered low or moderate concentration rHDL NPs revealed significant increases in dye

extraction when US therapy was utilized ($p < 0.05$) but not in animals dosed with the high concentration rHDL NPs ($p = 0.24$), Figure 7. Lastly, measurements of the dye extracted from excised tumor samples was compared to *in vivo* optical measurements obtained immediately prior to euthanasia and results indicate a positive correlation for only those animals receiving the low concentration rHDL NPs ± US therapy ($R^2 > 0.43$, $p < 0.03$).

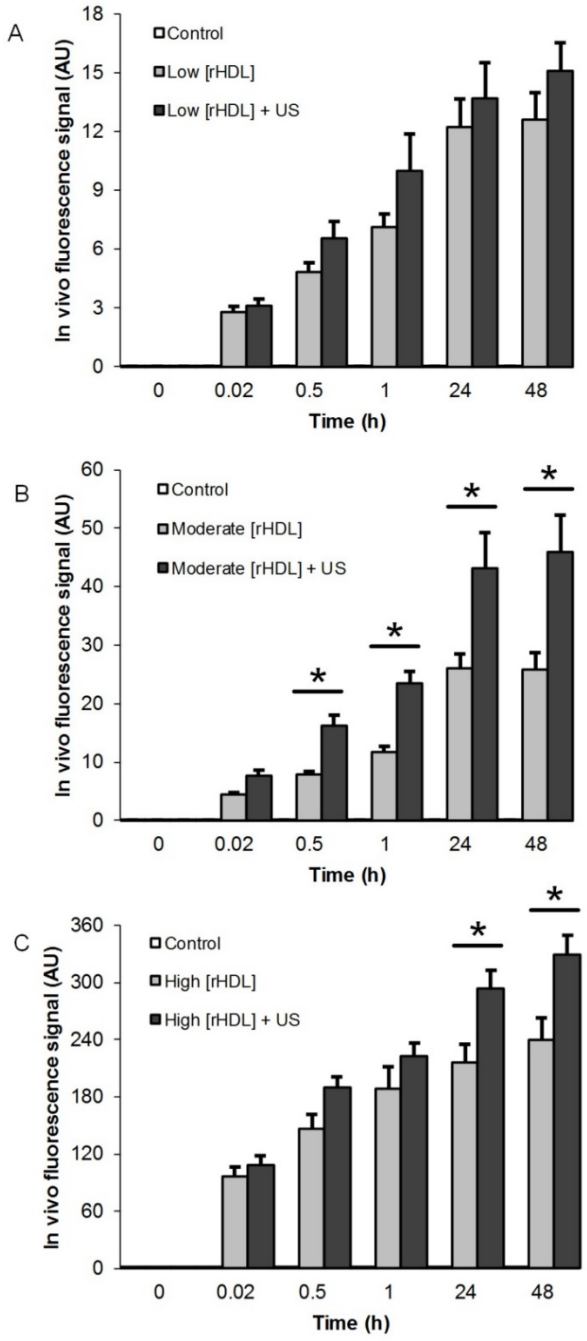

Figure 5. Summary of in vivo optical imaging results from breast tumor-bearing group animals administered either (A) low [rHDL] ± US therapy, (B) moderate [rHDL] ± US therapy, or (C) high [rHDL] ± US therapy at baseline, 1 min, 30 min, 60 min, 24 h and 48 h. Note the improved uptake of rHDL NPs at the target tumor site when noninvasive US is incorporated to the treatment protocol. A * indicates statistically significant differences.

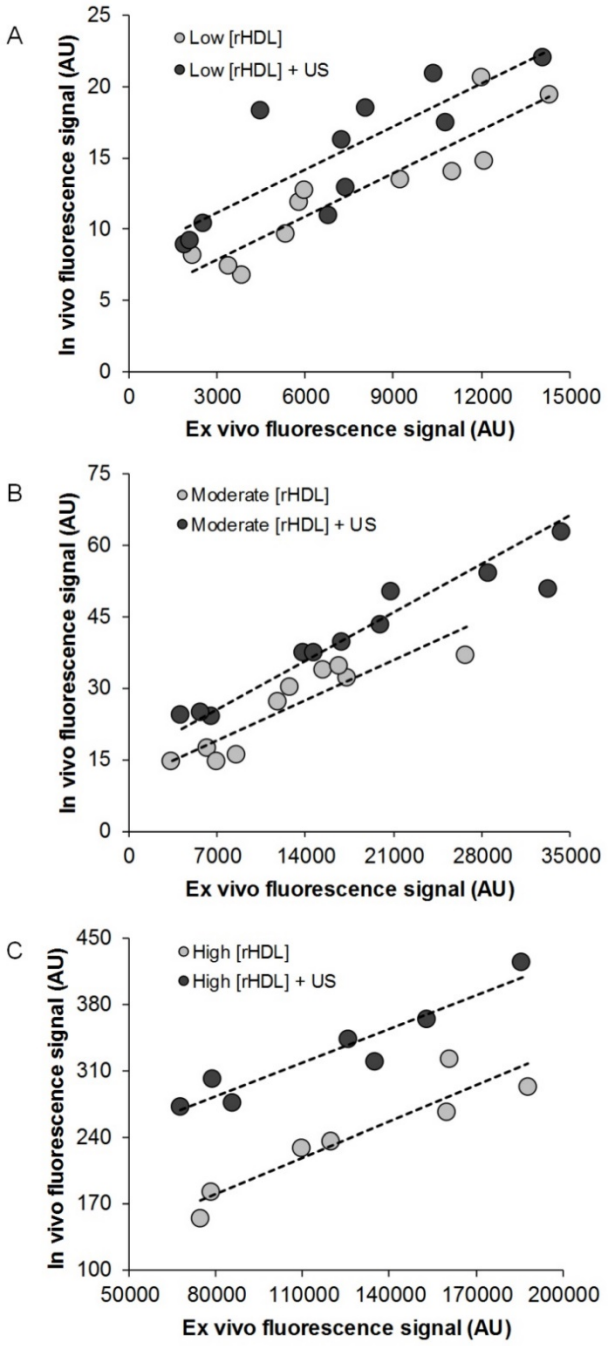

Figure 6. Scatterplot of *in vivo* and ex *vivo* optical imaging results at 48 h from breast tumor-bearing animals administrated either (A) low [rHDL] ± US therapy, (B) moderate [rHDL] ± US therapy, or (C) high [rHDL] ± US therapy. Trend lines (dashed) highlight the linear relationship between the tumor measurements.

Discussion

Drug-loaded rHDL NPs allow selective delivery of anticancer agents to tumors via the SR-B1 receptor, thus, unloading the drug payload from the rHDL NPs to cancer cells. To help achieve maximal benefit, the rHDL NPs must extravasate and locally accumulate in the tumor tissue space. To that end, US-stimulated drug delivery has considerable potential for

increasing localized rHDL NPs delivery in addition to a host of other clinical applications. As this novel US therapy continues to be explored, it is important to understand the effects and mechanisms of this adjunct to cancer therapy. In this study, we investigated the effects of US-stimulated drug delivery of IR-780 dye-loaded rHDL NPs in living animals. The overarching objective of this preliminary study was to investigate whether US-stimulated drug delivery of rHDL NPs can significantly improve tumor accumulation as compared to systemic injection of the rHDL NPs alone. Incorporation of an IR-780 dye into the rHDL NPs allowed us to study drug delivery longitudinally in living animals using a noninvasive optical imaging system.

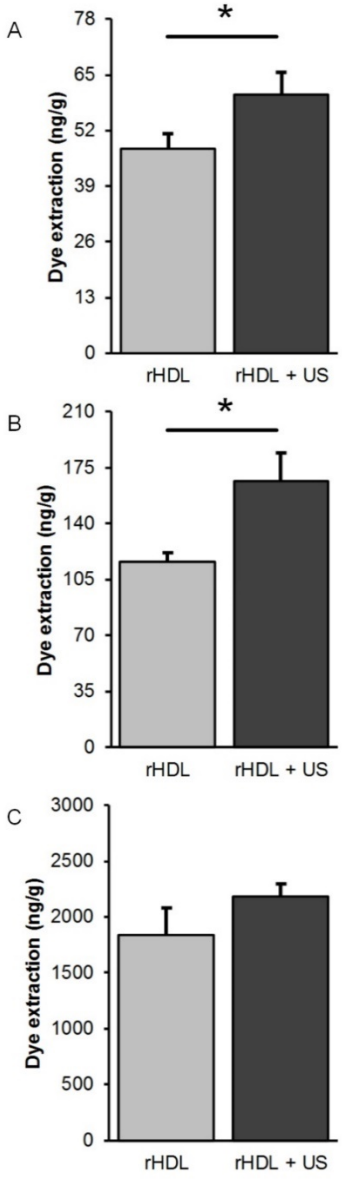

Figure 7. Comparison of IR-780 dye extraction data obtained from excised tumor samples at 48 h after exposure to (A) low [rHDL] ± US therapy, (B) moderate [rHDL] ± US therapy, or (C) high [rHDL] ± US therapy. A * indicates statistically significant differences.

A custom low intensity US therapeutic system (mechanical index = 0.45) was used to help minimize any disruption of tumor perfusion (29). Low intensity US exposure of systemically flowing MB contrast agents is known to temporarily enhance microvascular permeability in tumor tissue and improve delivery of any circulating anticancer drug. Thereafter, passive diffusion of the extravasated drug can result in better tumor treatment. By employing a continuous raster scan approach throughout the entire US exposure period, a limitation of this handheld US setup is that a complete and homogenous treatment of the tumor volume may have been conceded in addition to treatment of some surrounding healthy tissue. Nonetheless, during this study no change in optical imaging data was found in the control animals. However, there was considerable drug accumulation within 48 h in the low (5 μg), moderate (10 μg), and high (50 μg) rHDL NP concentration-dosed group animals ($p < 0.09$). With US therapy added to the experimental protocol, there was an additional and significant increase in local drug uptake at the tumor site ($p < 0.02$). While the early *in vivo* optical imaging sessions captured fluorescent signals from both intravascular and extravascular IR780-dye-loaded rHDL NPs, optical images acquired at 24 and 48 h reflected tumor fluorescence predominately due to the latter state given the circulating half-life of the rHDL NPs is only 12 to 24 h (30). Optical image data collected from *ex vivo* tumor samples confirmed tumor retention of the IR-780 dye-loaded rHDL NPs and correlated positively with *in vivo* optical imaging results ($R^2 > 0.69$, $p < 0.003$). While IR-780 dye extraction from the tumor tissue samples confirmed our *in vivo* and *ex vivo* US therapy findings, results were less consistent due to some basic concerns with the dye removal procedure and subsequent quantification. More specifically, we did not perform exsanguination of the animals before euthanasia and tumor extraction. Given the microvascular volume of these tumor tissues can contain a considerable amount of intravascular rHDL NPs, we believe this may have impeded an accurate *ex vivo* measurement of tumor retention (extravasation) by introducing a strong background signal. A noteworthy observation from the optical imaging data is that US-stimulated drug delivery using the lower dose of rHDL NP yielded the lowest gain (fluorescence signal increase) when compared to dosing with the IR-780 dye-loaded rHDL NPs alone. With the lower dose, we believe rHDL NP availability at the tumor site was limited because of the lower blood plasma concentration. Given the effect of light scattering on *in vivo* optical imaging can be significant, attenuation at tumor depth may have

impeded an accurate quantification of the IR-780 dye signal in larger tumors. Notwithstanding, this study highlighted the use of US-stimulated drug delivery for improving tumor treatment protocols and for offering the potential opportunity to use lower drug doses. As many anticancer chemotherapeutic agents can produce toxicity via off target effects, even at the approved therapeutic doses, improved (US-enhanced) drug delivery could have a major impact in both the adjuvant and neoadjuvant oncological setting.

A diverse collection of studies by our group and others have shown that intravascular MB contrast agents exposed to US energy can increase extravasation and enhance the susceptibility of malignant tissues to therapeutic agents (6, 11, 31-35). As shown in (3), changes in tumor microvascular permeabilization following US-stimulated drug delivery occurs within minutes and confirms the experimental findings presented herein. These tumor microvascular changes are known to be transient with homeostatic conditions typically returned within 48 h (29). This may help explain in part the slight plateauing of the data presented in Figure 5 (between 24 and 48 h). Given rHDL NPs are intrinsically targeted to cancer cells, one would expect to see continued drug accumulation at 48 h after the effects of US therapy have waned.

When exploring other *in vivo* applications of US-stimulated drug delivery, previously reported methods analyzed secondary indicators of tumor response to treatment by measuring physical size and evaluating histological results post-mortem (5, 6, 33, 36, 37). While monitoring changes in tumor size is an effective strategy for longitudinal studies, there is no immediate feedback for gauging the efficacy of the US enhanced therapeutic procedure. To that end, magnetic resonance imaging (MRI)-based measures have been explored and shown to be effective in confirming successful US-stimulated drug delivery in tumor tissue (29). Here the MRI image intensity after contrast injections is a function of the enhanced permeability and retention effect. After US therapy, this property allows circulating MR contrast agent to more selectively accumulate in tumor tissue compared to normal tissues. While effective, cost and image acquisition time considerations make the use of MRI challenging, especially in the preclinical research market. For monitoring US-stimulated drug delivery, noninvasive *in vivo* optical imaging is a cost-effective and versatile option. Over visible fluorescent dyes, advantages to optical imaging of dyes in the IR region is greater imaging depth, increased image resolution, and higher signal-to-background signal ratio (38). Results presented in Figure 4 further highlight the *in vivo* use of IR-780 dye-loaded rHDL NPs and the ability to be successfully localized in tumor tissue after application of US-stimulated drug delivery. Given the ever-expanding role of fluorescence imaging in human oncology (39, 40), the prospect of using this modality for monitoring US-stimulated drug delivery is encouraging. Future work will investigate the use of US-stimulated drug delivery of rHDL NPs preloaded with both an anticancer drug and IR-780 dye. A series of longitudinal preclinical studies will help optimize the drug dosing schedule and overall therapeutic protocol. These experiments should also include an evaluation of adjacent normal tissue toxicity proximal to the tumor masses compared to contralateral tissue.

Conclusion

This study produced encouraging preclinical results exploring the use of US-stimulated drug delivery using IR-780 dye-loaded rHDL NPs in the neoadjuvant setting for the improved treatment of breast cancer. On average, optical imaging results confirmed that the use of US therapy for only 30 min can significantly improves drug accumulation compared to a single systemic injection of the rHDL NPs alone. *In vivo* optical imaging results were positively correlated with *ex vivo* tumor tissue measurements. Overall, US-stimulated drug delivery is a promising technology and the incorporation of novel drug-loaded rHDL NPs may help improve cancer management by minimizing long-term complications and the number of invasive surgeries that patients are forced to endure.

Abbreviations

3D: 3-dimensional; ANOVA: analysis of variance (ANOVA); HDL: high-density lipoprotein; IR: infrared; MB: microbubble; NP: nanoparticle; ROI: region-of-interest; rHDL: reconstituted high-density lipoprotein; SR-B1: scavenger receptor type B1; US: ultrasound

Acknowledgements

The authors would like to thank Mouna Taroua, BS, for her help and assistance during the optical imaging studies. This work was supported in part by NIH grants K25EB017222 and R21CA212851, Texas CPRIT awards DP150091 and RR150010 and the Rutledge Foundation, Fort Worth, TX.

Competing Interests

The authors have declared that no competing interest exists.

References

1. Jain RK. Delivery of molecular and cellular medicine to solid tumors. Adv Drug Deliv Rev. 2012;64(Suppl):353-65.
2. Jain RK. Normalization of tumor vasculature: an emerging concept in antiangiogenic therapy. Science. 2005;307(5706):58-62.
3. Sorace A, Saini R, Rosenthal E, Warram J, Zinn K, Hoyt K. Optical fluorescent imaging to monitor temporal effects of microbubble-mediated ultrasound therapy. IEEE Trans Ultrason Ferroelectr Freq Control. 2013;60(2):281-9.
4. Sorace AG, Warram JM, Umphrey H, Hoyt K. Microbubble-mediated ultrasonic techniques for improved chemotherapeutic delivery in cancer. J Drug Target. 2012;20(1):43-54.
5. Heath CH, Sorace A, Knowles J, Rosenthal E, Hoyt K. Microbubble therapy enhances anti-tumor properties of cisplatin and cetuximab in vitro and in vivo. Otolaryngol Head Neck Surg. 2012;146(6):938-45.
6. Kotopoulis S, Delalande A, Popa M, Mamaeva V, Dimcevski G, Gilja OH, et al. Sonoporation-enhanced chemotherapy significantly reduces primary tumour burden in an orthotopic pancreatic cancer xenograft. Mol Imaging Biol. 2014;16(1):53-62.
7. Sirsi SR, Borden MA. Advances in ultrasound mediated gene therapy using microbubble contrast agents. Theranostics. 2012;2(12):1208-22.
8. Sirsi SR, Hernandez SL, Zielinski L, Blomback H, Koubaa A, Synder M, et al. Polyplex-microbubble hybrids for ultrasound-guided plasmid DNA delivery to solid tumors. J Control Release. 2012;157(2):224-34.
9. Sorace AG, Warram JM, Mahoney M, Zinn KR, Hoyt K. Enhancement of adenovirus delivery after ultrasound-stimulated therapy in a cancer model. Ultrasound Med Biol. 2013;39(12):2374-81.
10. Sirsi S, Borden M. Microbubble compositions, properties and biomedical applications. Bubble Sci Eng Technol. 2009;1(1-2):3-17.
11. Sorace AG, Korb M, Warram JM, Umphrey H, Zinn KR, Rosenthal E, et al. Ultrasound-stimulated drug delivery for treatment of residual disease after incomplete resection of head and neck cancer. Ultrasound Med Biol. 2014;40(4):755-64.
12. Kotopoulis S, Dimcevski G, Gilja OH, Hoem D, Postema M. Treatment of human pancreatic cancer using combined ultrasound, microbubbles, and gemcitabine: a clinical case study. Med Phys. 2013;40(7):072902.
13. Dimcevski G, Kotopoulis S, Bjånes T, Hoem D, Schjøtt J, Gjertsen BT, et al. A human clinical trial using ultrasound and microbubbles to enhance gemcitabine treatment of inoperable pancreatic cancer. J Control Release. 2016; 243:172-81.
14. Lund-Katz S, Phillips MC. High density lipoprotein structure-function and role in reverse cholesterol transport. Subcell Biochem. 2010; 51:183-227.
15. Lacko AG, Sabnis NA, Nagarajan B, McConathy WJ. HDL as a drug and nucleic acid delivery vehicle. Front Pharmacol. 2015; 6:247.
16. Lacko AG, Nair M, Prokai L, McConathy WJ. Prospects and challenges of the development of lipoprotein-based formulations for anti-cancer drugs. Expert Opin Drug Deliv. 2007;4(6):665-75.
17. Shah S, Chib R, Raut S, Bermudez J, Sabnis N, Duggal D, et al. Photophysical characterization of anticancer drug valrubicin in rHDL nanoparticles and its use as an imaging agent. J Photochem Photobiol B. 2016; 155:60-5.
18. Sabnis N, Lacko AG. Drug delivery via lipoprotein-based carriers: answering the challenges in systemic therapeutics. Ther Deliv. 2012;3(5):599-608.
19. Lacko AG, Nair M, Paranjape S, Johnso S, McConathy WJ. High density lipoprotein complexes as delivery vehicles for anticancer drugs. Anticancer Res. 2002;22(4):2045-9.
20. Steinberg D. A docking receptor for HDL cholesterol esters. Science. 1996;271(5248):460-1.
21. Connelly MA, Williams DL. SR-BI and HDL cholesteryl ester metabolism. Endocr Res. 2004;30(4):697-703.
22. Cruz PM, Mo H, McConathy WJ, Sabnis N, Lacko AG. The role of cholesterol metabolism and cholesterol transport in carcinogenesis: a review of scientific findings, relevant to future cancer therapeutics. Front Pharmacol. 2013; 4:119.
23. Wang Y, Liu T, Zhang E, Luo S, Tan X, Shi C. Preferential accumulation of the near infrared heptamethine dye IR-780 in the mitochondria of drug-resistant lung cancer cells. Biomaterials. 2014;35(13):4116-24.
24. Yi X, Yan F, Wang F, Qin W, Wu G, Yang X, et al. IR-780 dye for near-infrared fluorescence imaging in prostate cancer. Med Sci Monit. 2015; 21:511-7.
25. Yang X, Shi C, Tong R, Qian W, Zhau HE, Wang R, et al. Near IR heptamethine cyanine dye-mediated cancer imaging. Clin Cancer Res. 2010;16(10):2833-44.
26. Sabnis N, Nair M, Israel M, McConathy WJ, Lacko AG. Enhanced solubility and functionality of valrubicin (AD-32) against cancer cells upon encapsulation into biocompatible nanoparticles. Int J Nanomedicine. 2012; 7:975-83.
27. McConathy WJ, Nair MP, Paranjape S, Mooberry L, Lacko AG. Evaluation of synthetic/reconstituted high-density lipoproteins as delivery vehicles for paclitaxel. Anticancer Drugs. 2008;19(2):183-8.
28. Hoyt K, Umphrey H, Lockhart M, Robbin M, Forero-Torres A. Ultrasound imaging of breast tumor perfusion and neovascular morphology. Ultrasound Med Biol. 2015;41(9):2292-302.
29. Sorace A, Hoyt K. Imaging the microvascular response to ultrasound-stimulated therapy in a preclinical animal model of breast cancer. Proc IEEE Ultrasonics Sympos. 2014:2145-8.
30. Kuai R, Li D, Chen YE, Moon JJ, Schwendeman A. High-Density Lipoproteins: Nature's Multifunctional Nanoparticles. ACS Nano. 2016;10(3):3015-41.
31. Zhao YZ, Dai DD, Lu CT, Lv HF, Zhang Y, Li X, et al. Using acoustic cavitation to enhance chemotherapy of DOX liposomes: experiment in vitro and in vivo. Drug Dev Ind Pharm. 2012;38(9):1090-8.
32. Cao WJ, Matkar PN, Chen HH, Mofid A, Leong-Poi H. Microbubbles and ultrasound: Therapeutic applications in diabetic nephropathy. Adv Exp Med Biol. 2016; 880:309-30.
33. Mullick Chowdhury S, Wang TY, Bachawal S, Devulapally R, Choe JW, Abou Elkacem L, et al. Ultrasound-guided therapeutic modulation of hepatocellular carcinoma using complementary microRNAs. J Control Release. 2016; 238:272-80.
34. Wood AK, Sehgal CM. A review of low-intensity ultrasound for cancer therapy. Ultrasound Med Biol. 2015;41(4):905-28.
35. Hauff P, Seemann S, Reszka R, Schultze-Mosgau M, Reinhardt M, Buzasi T, et al. Evaluation of gas-filled microparticles and sonoporation as gene delivery system: feasibility study in rodent tumor models. Radiology. 2005;236(2):572-8.
36. Gerst S, Hann LE, Li D, Gonen M, Tickoo S, Sohn MJ, et al. Evaluation of renal masses with contrast-enhanced ultrasound: initial experience. AJR Am J Roentgenol. 2011;197(4):897-906.
37. Sorace A. Microbubble-mediated ultrasound therapy for enhanced drug delivery in cancer. University of Alabama at Birmingham. 2013.
38. Frangioni JV. In vivo near-infrared fluorescence imaging. Curr Opin Chem Biol. 2003;7(5):626-34.
39. Tipirneni KE, Rosenthal EL, Moore LS, Haskins AD, Udayakumar N, Jani AH, et al. Fluorescence imaging for cancer screening and surveillance. Mol Imaging Biol. 2017.
40. Rosenthal EL, Moore LS, Tipirneni K, de Boer E, Stevens TM, Hartman YE, et al. Sensitivity and specificity of Cetuximab-IRDye800CW to identify regional metastatic disease in head and neck cancer. Clin Cancer Res. 2017.